Resistivity of boron-doped diamond microcrystals

M. D. Jaeger, S. Hyun, A. R. Day,[a] M. F. Thorpe, and B. Golding[b]
Department of Physics and Astronomy and Center for Sensor Materials, Michigan State University, East Lansing, Michigan 48824-1116

(Received 5 January 1998; accepted for publication 11 March 1998)

We describe measurements of the electrical resistivity of micron-size crystallites of boron-doped diamond. Electron-beam lithography was employed for writing sample-specific contacts on small, well-faceted diamond crystals grown by chemical-vapor deposition on silicon substrates. After generating a three-dimensional computer model of the crystallite, a finite-element analysis was used to calculate the internal electrostatic potential distribution. Multiterminal resistance measurements, in conjunction with a computed geometrical factor, enabled the absolute resistivity to be determined. We find that the resistivities obtained from two different crystallites agree to better than 10%. The results are compared with transport measurements on a large-area homoepitaxial diamond film grown simultaneously with the crystallites. This method can be generalized to obtain electrical transport properties of other small, irregularly shaped samples. © *1998 American Institute of Physics.* [S0003-6951(98)02819-8]

The electronic properties of homoepitaxial diamond have been studied extensively,[1,2] but measurements on single-crystal diamond films grown on nondiamond substrates such as Si have not yet been possible. We present a description of methods developed for electrical transport measurements on arbitrarily shaped micron-size single crystals. The techniques involve a lithographic process for forming electrical contacts to as-grown crystallites, electrical transport measurements, and a numerical finite-element analysis (FEA) of potential distributions. The microcrystal contact technique employs a sequence of electron-beam lithography (EBL) steps, a planarization step, and high-temperature processing to develop low-resistance electrical contacts. EBL provides submicron contact features and alignment and is sufficiently flexible to accommodate varied crystallite shapes and electrode patterns. The FEA allows us to compute the potential within the three-dimensional crystallites, thus yielding the bulk resistivity as well as contact resistances from two-, three-, and four-terminal resistance measurements. A preliminary account of this method appears in Ref. 3. We demonstrate this approach on isolated single crystals of boron-doped CVD diamond with dimensions of a few μm grown on oxidized-Si substrates. We compare these results with those obtained on a simultaneously deposited homoepitaxial diamond film.

The substrates for the diamond crystallites were Si wafers with a 4 μm thick oxidation layer. The substrates were lightly abraded with 0.1 μm diamond particles and the debris subsequently removed with ultrasonic scrubbing in acetone. The resulting nucleation densities were $<10^5$ cm^{-2}, which yielded well-isolated crystallites. Boron-doped diamond was grown using microwave plasma-assisted CVD and bias-enhanced nucleation with diborane gas as a boron source.[4] Isolated microcrystals averaged 4 μm in lateral dimensions and 2 μm in height. They exhibited primarily (111) and (100) facets, but were randomly oriented and occasionally twinned.

As-deposited diamond films were electrochemically etched[5] to remove surface graphite and then etched in a solution of HCl and H_2O_2.[6] Scanning electron micrographs recorded the location and orientation of isolated crystals, selected with a large top facet parallel to the substrate. Alignment marks were created on the substrate near each crystallite to facilitate subsequent feature alignment to within 0.2 μm. Thick PMMA resist (2 μm) ensured that the tops of the crystallites were adequately protected during initial alignment and subsequent metallization.

EBL was used to create contact pads on the top facets of the selected crystallites. Contact pads were, typically, 0.3 μm square and were metallized by thermal evaporation with 17 nm Ti and 100 nm Au. The samples were then annealed for 1 h at 650 °C in a nominally UHV system. The annealing produces a solid-state reaction between the Ti and the diamond, which reduces the Schottky barrier at the contact.[7] The crystallites and contacts of each microcrystal were then recorded by SEM micrographs taken at several angles.

Next, the crystallite was planarized by spin applying a 2.5 μm layer of electrically insulating polyimide,[8] which completely covered the crystallites and smoothed out steps in the surface profile. The polyimide was lightly cured for 3.5 h under an infrared lamp and then isotropically wet etched in diluted Shipley MF-319 photoresist developer so that the contact pads and the tops of the crystallites were completely exposed. The polyimide was then cured by baking at 140 °C for 1 h. The resulting polyimide layer provided a planarized surface to promote uniform resist thickness for subsequent EBL steps and to fill in crystallite undercuts, which would otherwise produce shadowing during lead metallization. EBL was then used to pattern 200 nm thick Au leads on top of the polyimide to contact the Ti/Au contact pads. Macroscopic pads were formed to which 25 μm diam Au wires were connected using silver paint. Figure 1 is a schematic profile

[a] Permanent address: Department of Physics, Marquette University, Milwaukee, WI 53233.
[b] Electronic mail: golding@pa.msu.edu

 © 1998 American Institute of Physics
Downloaded 30 Jul 2004 to 143.105.8.12. Redistribution subject to AIP license or copyright, see http://apl.aip.org/apl/copyright.jsp

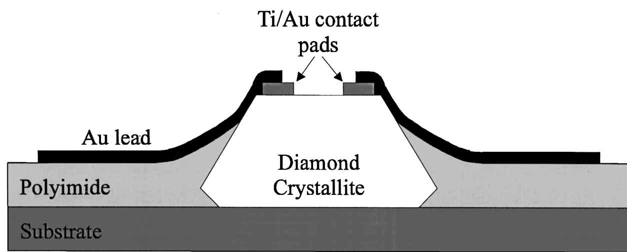

FIG. 1. Schematic cross section of a contacted diamond microcrystal, showing annealed Ti/Au contact pads, insulating polyimide planarization layer, and conformal Au leads.

of a completed crystallite. Figure 2 is a side-view SEM of a contacted crystallite, showing Au leads following the tapered polyimide to the top of the crystallite, where they overlap the Ti/Au contact pads.

For comparison with a regular morphology, a large-area homoepitaxial diamond film was grown simultaneously with the microcrystals on a (100) type-IIa diamond substrate. The film covered a 3 mm square area with a thickness of 1.86 μm. Four Ti/Au contact pads 300 μm square in the corners of the film were defined by EBL and processed in the same way as the microcrystal contacts. Au wires were connected directly to the pads by silver paint. The four-probe dc conductance was measured as a function of temperature for the homoepitaxial film and for two microcrystals, designated A and B. Four-terminal $I-V$ characteristics were linear over the temperature range of resistance measurements, 200–440 K, at $\leqslant 0.2$ V applied voltages. The temperature-dependent four-terminal resistances of all samples showed a change of several orders of magnitude within 100° of room temperature and exhibited nearly the same slope.

The physical quantity of primary interest is the geometry-independent resistivity of each sample. By assuming a spatially uniform and isotropic resistivity ρ, one can relate a four-terminal resistance measurement to the resistivity by $R_{ij}^{lm}=\rho\Gamma_{ij}^{lm}$, where the shape-dependent numerical factor Γ_{ij}^{lm} is a function of the measurement geometry. Here, subscripts are associated with current leads I_i and I_j and voltage probes V_l and V_m for a multiterminal resistance de-

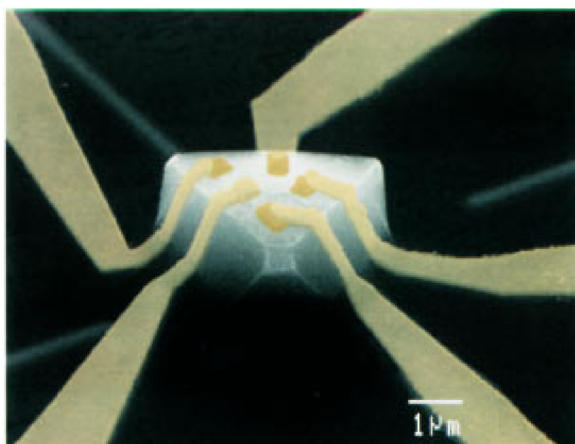

FIG. 2. 45° side-view SEM of a diamond microcrystal showing Au leads on top of a planarizing polyimide layer. The leads overlap Ti/Au contact pads on top of the crystallite. The bottom edges of the crystallite and the Ti/Au alignment marks (straight diagonal lines) are buried underneath the polyimide.

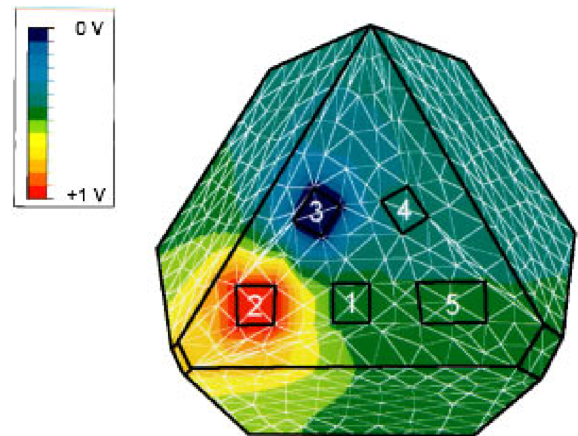

FIG. 3. Computed potential distribution on the surface of the contacted crystallite A (Fig. 2) for current contacts 2 and 3. The scale spans a potential difference of 1 V.

fined by $R_{ij}^{lm}=V_{lm}/I_{ij}$.[9] For quasi-two-dimensional samples with edge contacts, the van der Pauw technique,[10,11] based on conformal mapping, provides a method for determining the geometrical factor, and hence, the resistivity. It cannot be used to interpret the resistance measurements on diamond microcrystallite samples, however, since they are highly three-dimensional (3D), with aspect ratios near unity. To accommodate such irregular shapes, a numerical technique for calculating the geometrical factors for multiprobe resistance measurements on arbitrarily shaped objects with uniform resistivity was developed.[9]

The geometrical shape of each crystallite was reconstructed from SEM micrographs of the crystallite from at least five different viewing directions. The images were digitized and the vertex coordinates of facet and contact pad corners determined. The scale, coordinates, and viewing angles for each photograph were input into a least-squares routine which returned the optimized coordinates for the crystallite and contacts.[9] For well-shaped crystallites with observably flat facets, the refined angles between facets agreed with the ideal angles to within 1°.

FEA[12] was used to calculate the potential distribution and to obtain the geometrical factors for the refined crystal shape and contact pads. The number of total volume elements used in the FEA was, typically, 3000, and smaller mesh sizes did not significantly degrade the results. The procedure solves Laplace's equation $\nabla^2\Phi(x,y,z)=0$ within each volume element subject to the boundary conditions that no current flows into or out of the sample boundary except at the contacts, and that the contact pads are perfect conductors at constant potential. The output of the FEA is the value of the potential at each mesh node and the value of the multiterminal resistance normalized to unit conductivity Γ_{ij}^{lm}. Fig. 3 shows the calculated potential distribution on the surface of crystallite A, along with the FEA mesh, for the case in which a voltage is applied across contacts 2 and 3.

The resistivity from the i four-terminal resistance measurements was determined by first minimizing the function $\Sigma_i(R_i^e-R_i^t(\rho))^2$, where R_i^e are the experimentally measured resistances and $R_i^t(\rho)=\rho\Gamma_i$ are the calculated resistances, and ρ is the resistivity. In practice, the geometrical factor was obtained from six four-terminal measurements. The analysis,

Downloaded 30 Jul 2004 to 143.105.8.12. Redistribution subject to AIP license or copyright, see http://apl.aip.org/apl/copyright.jsp

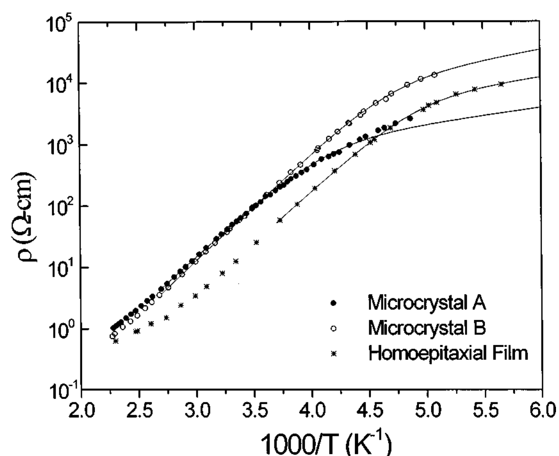

FIG. 4. Resistivity of B-doped diamond microcrystals and a simultaneously grown homoepitaxial film. Solid lines are least-squares fits of the data to a model for lightly doped semiconductors $\rho^{-1}=\sigma=\sigma_1\exp(-E_1/k_BT)+\sigma_2\exp(-E_2/k_BT)$.

described in greater detail elsewhere,[9] was carried out for samples A and B and for a homoepitaxial film. For the film, we checked the values calculated from the van der Pauw formula against the full calculation and found agreement to 5.5%. The absolute resistivities of the two microcrystals agree to within 10% at room temperature, despite differences in their shapes and contacts. This confirms the correctness of the geometrical model and electrostatic calculation. However, the resistivities of the microcrystallites are nearly three times greater than the homoepitaxial film at this temperature.

Figure 4 shows the temperature dependence of the resistivities. All samples exhibit the same temperature dependence near 300 K. Below room temperature, deviations in the resistivity from valence-band transport are believed to represent sample-specific characteristics arising from the presence of localized states. For lightly doped p-type semiconductors, the conductivity is often represented as a sum of terms $\sigma=\sigma_1\exp(-E_1/k_BT)+\sigma_2\exp(-E_2/k_BT)$, where the first term corresponds to valence-band hole conduction with activation energy E_1 and the second term corresponds to nearest-neighbor hopping between boron acceptor sites.[13] E_1 is approximately the impurity ionization energy. The dominant conduction mechanism shifts from the valence-band conduction at intermediate temperatures to the hopping conduction at low temperatures since E_1 is larger than E_2. We fit the data with σ_1, E_1, σ_2, and E_2 as parameters over a limited range of temperature, assuming that mobility changes are inconsequential. The results are shown as solid lines in Fig. 4. The model accurately describes the data with the exception of sample A at the lowest temperatures where non-Ohmic conduction processes set in. The values of $E_1=0.34\pm0.01$ eV are in good agreement for microcrystals and homoepitaxial film. This indicates that the environment for boron acceptors is the same in deposited homoepitaxial diamond grown on (100) single-crystal type-IIa natural diamond.

The Hall resistance for the homoepitaxial film was measured in perpendicular magnetic fields up to 1 T using the van der Pauw method.[11] We find a Hall mobility of 550 cm^2/V s at room temperature, in good agreement with similarly prepared films. This yields a hole concentration of 1×10^{16} cm^{-3} and an acceptor density N_A of 1.2×10^{18} cm^{-3}.

The factor of 3 resistivity difference between the microcrystals and the homoepitaxial film requires further comment. Reports[14] of higher dopant incorporation rates for (111)-faceted growth compared to (100)-faceted growth predict that, since the microcrystals exhibit both facet types and the homoepitaxial film is primarily (100) faceted, the microcrystals should have higher dopant concentrations, and thus, lower resistivity compared to the homoepitaxial film. This prediction is contrary to our observations. A likely explanation of the observed resistivity difference is that the dopant concentrations are similar, but the microcrystals possess a lower hole mobility ($\mu=1/n_he\rho$, where n_h is the carrier concentration) due to a higher defect density. Such defects could perhaps be Si impurities incorporated from the substrate during growth.

In summary, we have described lithographic methods for contacting microcrystals, a numerical technique based on finite-element analysis for interpreting resistance measurements, and its application to irregularly shaped 3D diamond. These methods can be readily adapted to other materials for which large size or regular samples are not available.

The authors thank H. Wynands at Kobe Steel USA for useful discussions. The support of the NSF through the Center for Sensor Materials MRSEC DMR 94-00417 as well as DMR 93-12544 is gratefully acknowledged.

[1] E. P. Visser, G. J. Bauhuis, Ger Janssen, W. Vollenberg, W. J. P. van Enckevort, and L. J. Giling, J. Phys.: Condens. Matter **4**, 7365 (1992).
[2] D. M. Malta, J. A. von Windheim, H. A. Wynands, and B. A. Fox, J. Appl. Phys. **77**, 1536 (1995).
[3] M. D. Jaeger, S. Hyun, A. R. Day, M. F. Thorpe, and B. Golding, Diamond Relat. Mater. **6**, 325 (1997).
[4] Diamond grown at Kobe Steel USA Inc., Electronic Materials Center, 79 T. W. Alexander Drive, P.O. Box 13608, Research Triangle Park, NC 27709.
[5] M. Marchywka, P. E. Pehrsson, S. C. Binari, and D. Moses, J. Electrochem. Soc. **140**, L19 (1993).
[6] D. K. Reinhard, *Introduction to Integrated Circuit Engineering* (Houghton Mifflin, Boston, MA, 1987), p. 388.
[7] T. Tachibana and J. T. Glass, in *Diamond: Electronic Properties and Applications*, edited by L. S. Pan and D. R. Kania (Kluwer, Norwell, MA, 1995), pp. 319–48.
[8] We used PYRALIN PI-2555 polyimide coating and VM-651 adhesion promoter supplied by DuPont.
[9] S. Hyun, M. F. Thorpe, M. D. Jaeger, B. Golding, and A. R. Day, Phys. Rev. B **57**, 6697 (1998).
[10] L. J. van der Pauw, Philips Res. Rep. **13**, 1 (1958).
[11] K. Seeger, *Semiconductor Physics, An Introduction* (Springer, New York, 1991), pp. 62–3.
[12] Finite-element analysis packages used were ABAQUS and ANSYS. ANSYS is a registered trademark of ANSYS, Inc., Southpointe, 275 Technology Drive, Canonsburg, PA 15317. ABAQUS is the product of Hibbitt, Karlsson, and Sorensen, Inc., 1080 Main Street, Pawtucket, RI 02860-4847.
[13] B. I. Shklovskii and A. L. Efros, *Electronic Properties of Doped Semiconductors* (Springer, Berlin, 1984), Chap. 4.
[14] A. T. Collins, Philos. Trans. R. Soc. London, Ser. A **342**, 233 (1993).

Downloaded 30 Jul 2004 to 143.105.8.12. Redistribution subject to AIP license or copyright, see http://apl.aip.org/apl/copyright.jsp